

Traffic State Estimation on Urban Roads Using Perception-Enriched Floating Car Data

Moritz Schweppenhäuser¹ ^a, Karl Schrab² ^b, Robert Protzmann¹ ^c and Ilja Radusch²

¹Fraunhofer Institute FOKUS, Kaiserin Augusta Allee 31, 10589 Berlin, Germany

²TU Berlin / Daimler Center for Automotive IT Innovations, Ernst-Reuter-Platz 7, 10587 Berlin, Germany

Keywords: Traffic State Estimation, Simulation, Vehicle Perception, Eclipse MOSAIC.

Abstract: Modern-day navigation systems by developers like Google© and TomTom© require user participation primarily in the form of Floating Car Data (FCD) for accurate Traffic State Estimation (TSE). However, to provide reliable information, systems rely on large road user participation of at least 5 %, which is only truly available to the big players. We propose a method to soften the participation requirement by utilizing modern perception sensors (e.g., radar, lidar, camera) of connected vehicles (CVs) to enrich the FCD set, compensating reduced data quantity with increased data quality. By using position and speed estimates of surrounding vehicles we increase the sample size and can additionally collect estimates of segments that are not traversed by CVs. To validate and assess the proposed system, we utilize Eclipse MOSAIC and conduct a simulation-based test series on the calibrated large-scale BeST scenario. Initial findings indicate improved estimation performance on selected road segments, especially at lower rates of market penetrations. In a network-wide investigation, we show that travel time estimates of the proposed method are often more accurate than conventional approaches, while also requiring smaller penetration rates.

1 INTRODUCTION

In a world highly dependent on personal mobility, traffic congestion is a daily issue, leading to wasted time, increased emissions, and fuel consumption. Navigation system developers try to alleviate the traffic strain by providing real-time Traffic State Estimation (TSE) for users, giving them the ability to avoid traffic build-ups and congested areas. To provide accurate estimations, current-day systems typically rely on large amounts of data provided by users. This data is referred to as Floating Car Data (FCD) and is usually made up of a vehicle's position, its heading, and speed. This technology has been established over the last three decades and nowadays is an essential part of most navigation applications.


At the same time, automotive sensor technologies evolved to add richer perception sensors, such as radar, lidar, and cameras. This trend has been driven by advanced driver assistance systems and autonomous driving technology, reaching a state where


many new car models are equipped with such sensors.


In related work, Deloos et al. (Deloos et al., 2020) utilize V2X (vehicle-to-everything) communication to share the advanced sensor data between vehicles or servers to enable innovative use cases. This field of research is mainly driven by safety use cases such as collective perception.

Inspired by these use cases, we want to investigate the shared sensor output as an input for traffic efficiency applications. Specifically, we propose a TSE system that extends FCD packages with information about surrounding vehicles, including the respective position, heading, and speed. With this approach, we aim to further reduce market penetration thresholds of conventional FCD-based systems, potentially allowing smaller competitors to enter the market.

Similarly, Messelodi et al. (Messelodi et al., 2009) propose to enrich FCD with data from sensors on the equipped vehicles. Their approach includes warning sign recognition as well as a local traffic level estimator, relying on onboard preprocessing. Ruppe et al. (Ruppe et al., 2012) further propose to augment FCD with data from surrounding Bluetooth/Wi-Fi enabled devices, increasing the amount of collected data without the use of perception sensors.

^a  <https://orcid.org/0009-0001-9252-2425>

^b  <https://orcid.org/0000-0002-5083-595X>

^c  <https://orcid.org/0000-0002-5531-1936>

The work presented in this paper is built on previously published research, which gave an initial review on sensor modalities and aggregation methods for mean speed estimation (Schweppenhäuser et al., 2023). We extend the established system and test the novel solution using the co-simulation framework Eclipse MOSAIC (Schrab et al., 2023).

This paper is structured into four main sections. First, in Section 2 we reiterate fundamental requirements in terms of TSE relevant to this paper and explain how one could include potentially lossy data from surrounding vehicles. Secondly, we explain how we approach the implementation and deployment of the system in a simulated environment in Section 3. Conducted experiments and compiled results are described in Section 4. Finally, with Section 5 we lay out closing remarks and future research directions.

2 MEAN SPEED ESTIMATION

Estimating traffic flows, speeds, and densities has long been an important topic in traffic research. In real-world applications, this task quickly becomes difficult as only limited measurement options exist, each coming with different coverage, reliability, and costs. Historically, static observers such as induction loop sensors and traffic cameras have been deployed on major road arteries to investigate their traffic state with good accuracy. However, these static installations are costly which inherently limits their network coverage. Contrarily, the idea of using mobile sensors in the form of connected vehicles (CV), has been proposed as early as the 1950s (Wardrop and Charlesworth, 1954) using the “Moving Observer

Method”. This method relies on vehicles being able to perceive vehicles in the opposing lanes, which is why it was never widely deployed, as required sensors were not available in the past. Later on, with the larger availability of mobile connectivity and the universal adoption of smartphones, the “Floating Car Observer Method”, i.e., using Floating Car Data, gained popularity as this enabled the possibility for almost every end user to act as a mobile sensor.

Navigation application developers such as Google© and TomTom© rely on FCD for Traffic State Estimation. However, for aspiring competitors, the FCD method is hardly applicable as large amounts of data are required, ranging to 5 % to 10 % market penetration (Ferman et al., 2005) even for estimations on highways. On urban roads, this matter is further complicated due to much higher variability in driver behavior and a more complex road layout.

Independent of the applied sensor technology, the task of traffic state estimation describes the reconstruction of different traffic indexes such as flows, densities, mean speeds, and other metrics built on the former based on potentially sparse sensor data. Blokpoel et al. (Blokpoel et al., 2010) describe an unambiguous list of such traffic metrics used for classifying the traffic state. Building on our previous work we continue focusing on mean speed estimates, as the speed is one of the core indexes and can be directly used in fastest-path routing algorithms.

To better understand the role of speeds in the traffic state so-called *Space-Time Diagrams* can help (see Figure 1). We, conventionally, plot the time on the abscissa and the space on the ordinate. Trajectories of individual vehicles are displayed as purple lines and the slope of a trajectory indicates a vehicle’s speed.

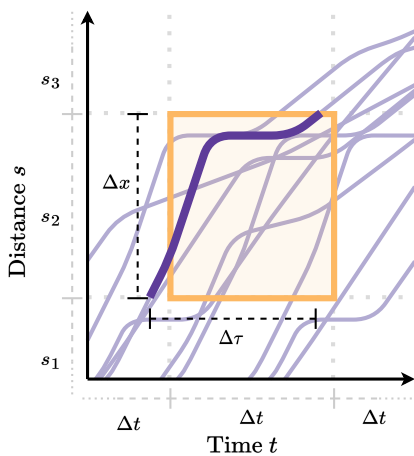


Figure 1: Exemplary space-time diagram in an urban scenario, highlighting large deviations in vehicle trajectories. The dark purple line indicates the calculation of the temporal mean speed for the marked spatio-temporal interval.

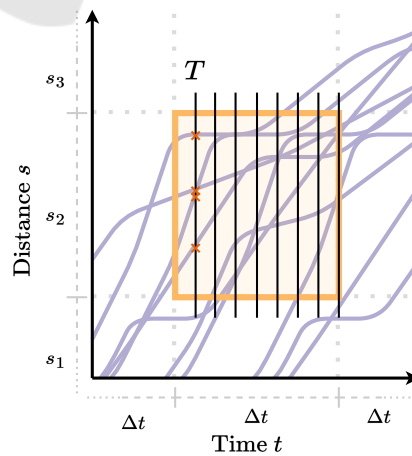


Figure 2: Depiction of how the sample-based mean speed is calculated for a given time interval Δt , where T indicates the set of all time steps within Δt . Each of the orange crosses indicates a sample recorded at the first time step.

Usually, one examines separate spatial and temporal intervals. Since the traffic state is a highly fluctuating measure precise estimations can only be made on a local scale, i.e., for certain time intervals (typically 5 min to 30 min) and on given streets or street segments. These intervals can be referred to as aggregation intervals and are indicated by the orange boxes.

Of course, if one has access to complete trajectories, the estimation of the average speed for a spatio-temporal interval would be as easy as calculating the arithmetic mean of all respective average speeds as shown in Equation (1).

$$V = \frac{1}{n} \sum_{i=0}^n \bar{v}_i = \frac{1}{n} \sum_{i=0}^n \frac{\Delta s_i}{\Delta t_i} \quad (1)$$

In reality, however, one deals with incomplete, potentially erroneous data and has to apply measures to fill in gaps and correct data. For position measurements, the most prominent fix is to apply Map-Matching (Brakatsoulas et al., 2005), which will fix Global Navigation Satellite System (GNSS) positions to the closest position on a digital map.

2.1 Interpolated Approaches

A conventional approach to mitigate the effect of incomplete FCD is to apply spline-based interpolation on the trajectory of the CVs. Yoon et al. (Yoon et al., 2007) establish the *Temporal Mean Speed* which is also visualized in Figure 1. The described method applies polynomial spline interpolation to reconstruct vehicle traversals. Based on the resulting splines the average velocity is calculated for each vehicle according to Equation (2).

$$v_{\text{temporal}} = \bar{v} = \frac{\Delta x}{\Delta \tau} \quad (2)$$

Even though this method delivers good results when using a large percentage of CVs and less frequent transmission of FCD, it quickly suffers in performance when decreasing market penetration, due to unsampled road segments.

2.2 Sample-Based Approaches

Opposing interpolated methods, it is also possible to treat received samples individually and calculate an averaged speed estimation that way. One such approach is displayed in Figure 2 which we label as the *Sample-based Mean Speed*. Here, we slice the spatio-temporal aggregation interval into equally sized time chunks called T . First, we average all speed values received for each time chunk T . Afterward, the arithmetic mean for the entire aggregation interval Δt is calculated following Equation (3).

$$v_{\text{sample}} = \frac{1}{T} \sum_{t=1}^T \left(\frac{1}{N} \sum_{\alpha=1}^N v_{\alpha}(t) \right) \quad (3)$$

While some information may be lost due to not inspecting trajectories, this approach offers the flexibility of integrating samples measured using other vehicles' perception sensors. Using this approach allows the integration of information from non-connected vehicles into the TSE, which otherwise would have only passively affected measurements. Figure 3 exemplarily highlights where the inclusion of perceived vehicles can be useful. These cases can roughly be categorized as follows:

1. **Flowing traffic:** Depending on the direction the perception sensors are facing, it is possible to add samples from vehicles moving in the same direction ($\hat{=}$ flowing) as the ego vehicle on all lanes of the driving direction. This information is less relevant for speed estimates, as other vehicles likely drive at similar speeds.
2. **Oncoming Traffic:** Front-facing perception sensors allow the integration of all vehicles on opposing lanes if there are no obstructions in the way. This information is highly valuable because it gives insights into the traffic state on opposing lanes correlates only minimally.
3. **Intersecting Traffic:** The speed information gathered at intersections has to be treated carefully as it rarely reflects the traffic state in its "flowing" state but more likely vehicles accelerating after waiting at a red light. Also, intersecting vehicles can easily be occluded.

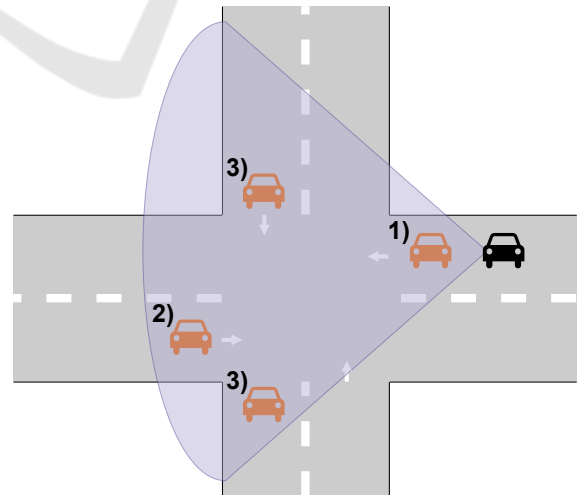


Figure 3: Illustration of additional samples acquired through the use of perception sensors. The black vehicle is a CV, while the orange vehicles can only be considered in the TSE due to the additional sensors.

3 SIMULATION APPROACH

As required sensor technologies are not broadly adapted yet and field tests are costly, we conduct our examinations in a simulated environment. Thus allowing us to implement and emulate all requirements for a complete system test in a cheap and fast manner. To ensure a degree of accountability and transferability we base the tests on domain-leading simulators that have independently stood the test of time.

3.1 Holistic Simulated Vehicle Perception and Data Fusion

For this paper, we do not aim toward mimicking a specific sensor technology and hardware requirements for our vehicle perception. Instead, we utilize the co-simulation framework Eclipse MOSAIC and its holistic perception model presented in (Protzmann et al., 2022). The perception model evaluates vehicle detections based on a circle sector defined by a radius r and an angle γ (see Figure 4).

While the applied model is a simplification of the perception task, it enables efficient simulation even of large-scale urban scenarios like the BeST-scenario (Schrab et al., 2022) and allows for assessing the general potential of the proposed TSE approach.

Coordinating data from many error-prone sources poses a challenge in real-world applications. Noisy measurements, timing offsets, and network obstructions (delay, jitter, package loss) hurt the fusion of samples. We deploy a server-side fusion of data that fuses samples by using the unique identifiers, which are sent as part of the FCD. Furthermore, we disregard timing and network effects entirely.

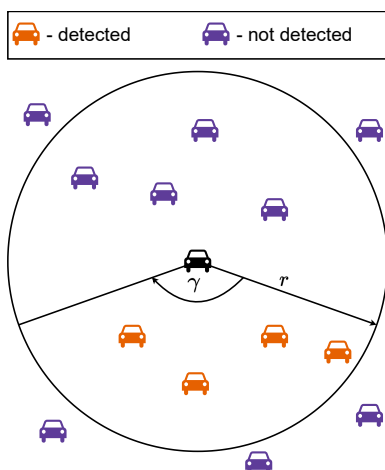


Figure 4: A simple depiction of the perception model applied in this paper using a field-of-view filter. Orange vehicles are detected while purple vehicles are not.

Realizing the system with these simplifications means we can only make limited prognoses on the performance of a real-world implementation. However, since we aim to evaluate the potential of a perception-enriched FCD, we will disregard these obstructions in this initial study. We furthermore, disregard privacy critical considerations but acknowledge the importance of secure obfuscation of user data.

3.2 Extended MOSAIC Applications

Simulation-based testing requires a strong foundation of realistic models to yield reliable results. Therefore, we utilize the well-established simulation framework Eclipse MOSAIC (Schrab et al., 2023) (see Figure 5), which is loosely based on the IEEE standard for High-Level Architecture (HLA) (Dahmann et al., 1997). MOSAIC couples many state-of-the-art FOSS simulators (Free and Open-Source Software) from different domains and also comes bundled with its own. One of the strong suits of MOSAIC is its powerful application simulator which enables fast testing of smart mobility applications, including V2X Communication via ITS-G5 and LTE/5G, autonomous vehicle perception, and e-mobility.

The applications utilized for this work are built on the application simulator and extend an openly available application suite (github.com/mosaic-addons/traffic-state-estimation), previously developed and published. These applications have been built to be easily extensible and allow for the integration of different sensor technologies on the vehicle side as well as extensibility in terms of TSE metrics on the server side.

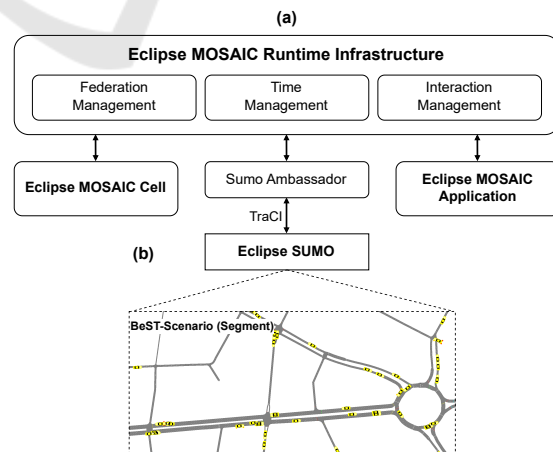


Figure 5: A rundown on Eclipse MOSAIC's architecture. (a) Runtime Infrastructure with the core tasks of federation, and time and interaction management, enabling a synchronized simulation. (b) Insight into the coupling of traffic simulator Eclipse SUMO including the BeST-scenario.

A basic schematic of the system design is depicted in Figure 6. The system is made up of two applications, one running on all CVs and one running on a centralized server. On the vehicle side, the *FCD Transmitter Application* will periodically collect FCD samples and transmit them in a collection called *FCD Update* to the *TSE Server* using MOSAIC’s bundled Cell simulator. In addition to conventional solutions, we extend the FCD with a list of all surrounding vehicles without any pre-processing for each connected vehicle (CV) using MOSAIC’s aforementioned perception model. The vehicle application can be configured with variable sample collection and update transmission times as well as perception ranges and angles.

At the heart of the server lies the *TSE Kernel*, which is responsible for receiving the FCD, extracting traversals, and supervising configured *FCD Processors*. Previously, the *Spatio-Temporal Traffic Metrics Processor* has been established which calculates the temporal and spatial mean speed as well as the Relative Traffic Status Metric (Yoon et al., 2007) from conventional FCD. The results from this processor are later used as a baseline. In a new development, we implemented the *Perception Metrics Processor* which additionally considers the added data from perception sensors. This processor aggregates the extended FCD in a two-stage approach. First, all retrieved samples are buffered using the time of collection as an index.

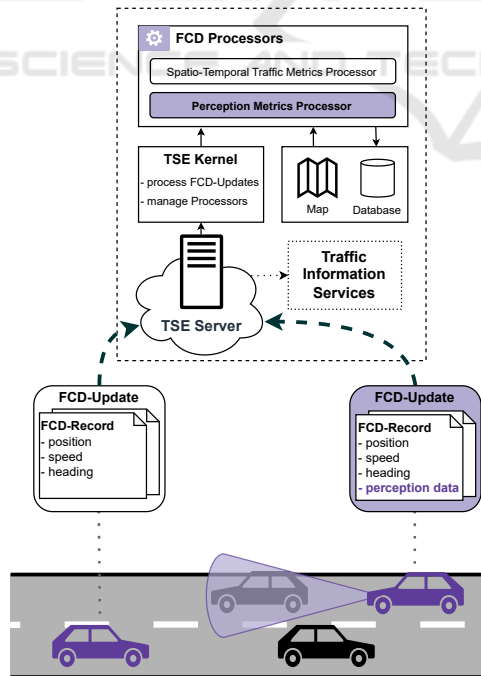


Figure 6: A simplified system overview of the applications. The top part depicts the structure of the server application and the bottom part shows how vehicles record FCD samples. The major new developments are marked in purple.

After a configurable delay, samples collected for the same vehicle at the same time will be averaged (i.e., being perceived by multiple other vehicles). We consider all samples as sharing the same truth regardless of their origin. After the configured delay, the aggregated samples for each vehicle will be moved to a secondary buffer that aggregates the samples per network edge, thus generating a mean speed estimate for each edge and time stamp. The results from this aggregation are then periodically persisted in a database for further post-processing and evaluation.

In a real-world deployment, the metrics would be relayed to Traffic Information Services to be accessible by end users. However, the evaluation of the data is conducted entirely offline, after simulation.

4 EVALUATION

In previous work, we presented a calibrated large-scale urban scenario for the city of Berlin (Schrab et al., 2022) for the traffic simulator Eclipse SUMO (Lopez et al., 2018) pre-configured to be used in-hand with MOSAIC. The scenario comprises an 800 km² road network, 24 hours of vehicular road traffic, and 2.25 million individual trips. For the evaluation of this paper, we opted to use the bundled subsection demand in the Charlottenburg area (see Figure 7), containing 200,000 trips, reducing simulation time immensely.

Utilizing MOSAIC’s Mapping Ambassador, we can equip variable percentages of the BeST traffic with our applications (Section 3.2). We assume *perfect* perception capabilities and configured vehicles with a 100 m viewing range and an angle of 360°, and also presume *perfect* communication capabilities ignoring effects of delay, packet loss, and jitter.

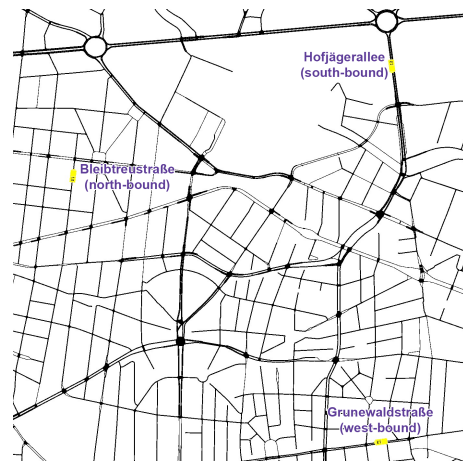


Figure 7: A map of Charlottenburg indicating the three street segments under examination.

Table 1: Key markers of the inspected road segments.

street segment	length	#lanes	speed limit	signalized
Hofjägerallee	399.96 m	3	50 $\frac{\text{km}}{\text{h}}$	no
Grunewaldstraße	185.37 m	2	50 $\frac{\text{km}}{\text{h}}$	yes
Bleibtreustraße	182.34 m	1	30 $\frac{\text{km}}{\text{h}}$	yes

As we are trying to improve on conventional TSE systems, which rely on 5 % to 10 % market penetration, we will further investigate rates below this threshold range. Additionally, we only look at the times from 6 am to 10 pm as the traffic volume outside this time window is insignificant, and a TSE becomes obsolete. In all following plots, we resample results into 15 min intervals using the arithmetic mean for mean speeds and summing up collected sample numbers.

4.1 Comparative Examination

In this first evaluation, we focus on the street segments on the Hofjägerallee, the Grunewaldstraße, and the Bleibtreustraße, highlighted in Figure 7. These street segments were also chosen in our previous work, due to exhibiting different characteristics that potentially impact the resulting mean speed estimates (see Table 1). The segment on the Hofjägerallee is a long segment with 3 lanes and no traffic light at the end resulting in a highway-like layout. The Grunewaldstraße can be classified as a larger urban street, with 2 lanes and a signalized end at the inspected segment. Lastly, the Bleibtreustraße is a lowly frequented, almost residential one-lane road that is also signalized.

Initially, we compare how the novel sample-based mean speed performs against conventional FCD-based approaches such as the temporal mean speed. For this, we create time-series plots for the penetration rates of 1 %, 2 %, 3 %, 5 %, 10 %, and 100 % as a baseline. Subsequently, we acquire plots in Figures 8, 10 and 12. In addition to the sample-based mean speed (orange) and the temporal mean speed (purple), we also plot the ground truth (GT) provided by SUMO as a baseline (gray). Furthermore, we create bar charts for the received samples on the server side in Figures 9, 11 and 13, to compare the received data based on applied market penetration for each the extended FCD (left-hand side) and the conventional FCD (right-hand side).

First, by comparing the temporal mean speed with the captured ground truth we can revalidate results from previous research. At 10 % and even 5 % market penetration, FCD-based TSE still delivers usable results on the larger Hofjägerallee and Grunewaldstraße

but fails on the smaller Bleibtreustraße. Interestingly, on the Hofjägerallee (Figure 8), the temporal mean speed still manages to deliver usable results when deploying only 1 % of CVs and only a few intervals go completely unsampled. This is mainly due to two reasons, (a) the Hofjägerallee is highly frequented and thereby likelihood of at least one CV-traversal every 15 min is fairly high, and (b) the variance of the realizable mean speed is low throughout the day and between different vehicles, which means that even one traversal can capture the mean speed accurately. The results for the Grunewaldstraße (Figure 10) start to degrade at higher market penetrations with many unsampled intervals at even 3 % and more outliers. We see increased over- and underestimations of the mean speed due to red traffic light phases either being captured or missed when fewer traversals are being aggregated in each interval. Lastly, the temporal mean speed fails to capture the mean speed at penetration rates of 5 % and lower for the Bleibtreustraße (Figure 12), as too few traversals are captured.

Next, looking at the resulting time series for the sample-based mean speed, some advantages but also some downfalls can be established. For the Hofjägerallee (Figure 8), a clear improvement is apparent compared to the temporal mean speed. Not only are we able to sample every interval even at 1 % penetration rate, but we also improve general consistency, capturing virtually zero outliers. The reasoning for this is similar to the reasons given for the good performance of the temporal mean speed. Capturing only a few additional samples of steady-flow traffic on a large, highly frequented road segment, allows for an improved TSE because most of the collected samples can be assumed to reflect the mean speed of the entire segment decently well. This effect cannot be observed in the same magnitude for the Grunewaldstraße and Bleibtreustraße. On the Grunewaldstraße (Figure 10), it is apparent that we can capture more and less fluctuating speed estimates using the sample-based mean speed even with penetration rates of about 2 %, meaning that the additional data from perception sensors do improve the overall quality of the estimates. Nonetheless, especially at lower penetration rates, the deviations from the ground truth are larger compared to the results on the Hofjägerallee.

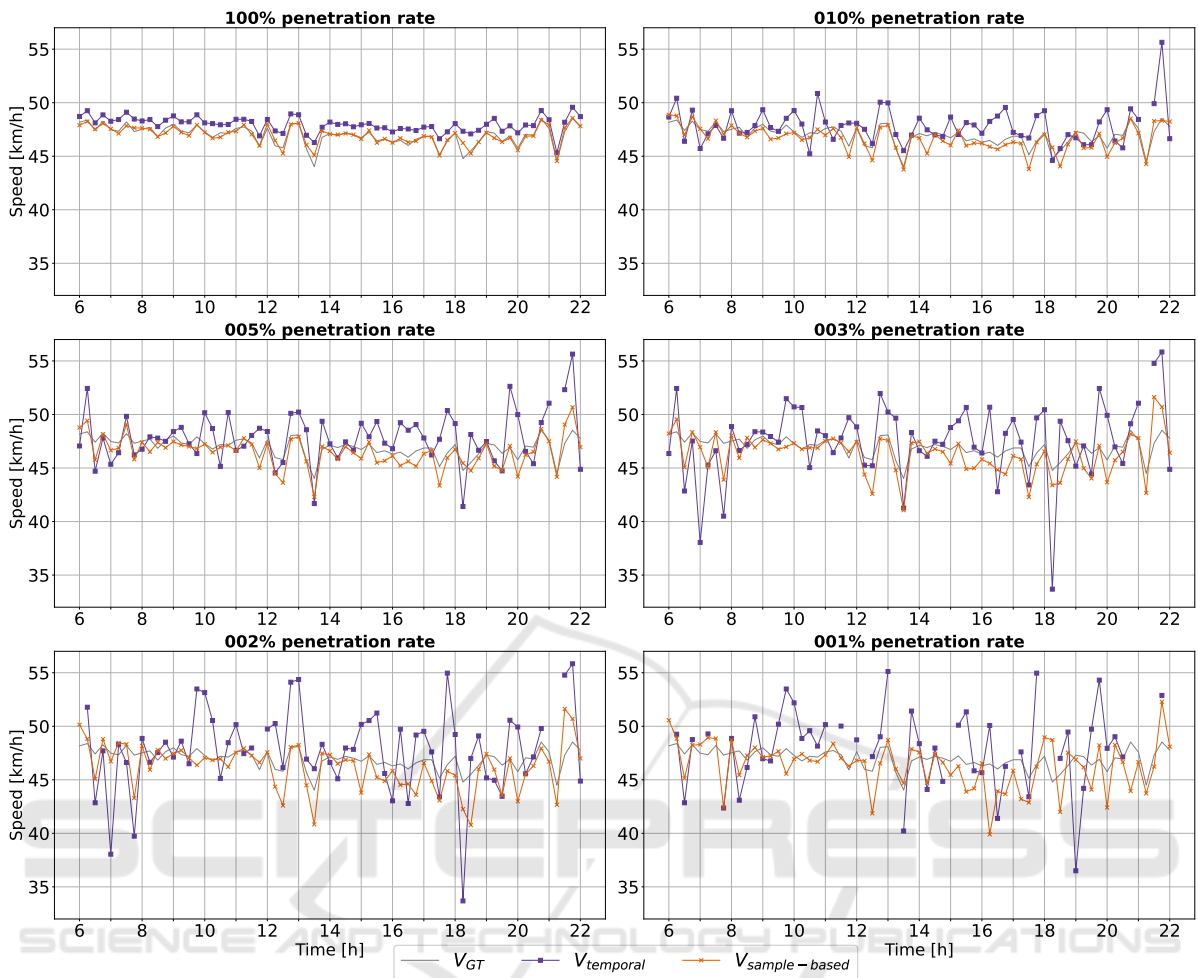


Figure 8: A comparison of the aggregated sample-based mean speed against the temporal mean speed on the Hofjägerallee. The values are measured for different penetration rates and averaged for 15 min intervals.

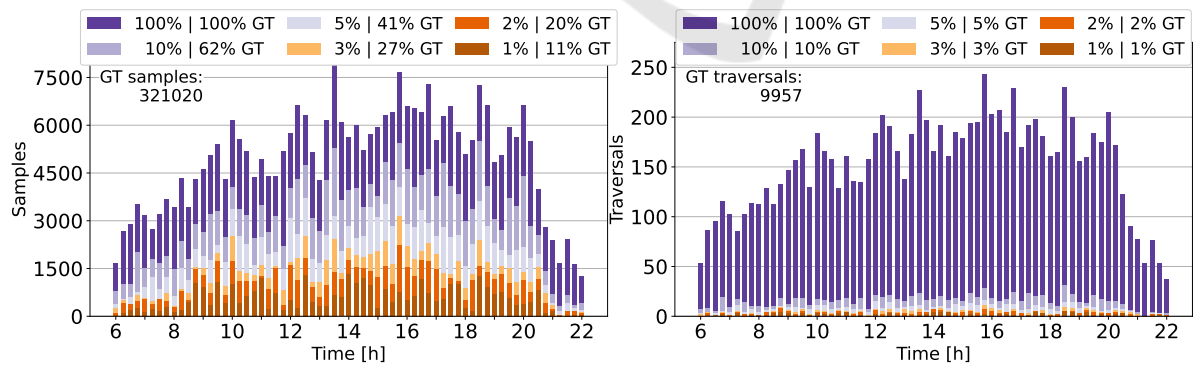


Figure 9: Comparison of received data amount depending on the rate of connected vehicles on the Hofjägerallee summed-up within 15 min intervals. **Left:** The number of individual samples (i.e., the sum of vehicles per road segment each time step) used for the sample-based mean speed using conventional FCD plus perception. **Right:** The number of extracted traversals used for the temporal mean speed, relying solely on conventional FCD.

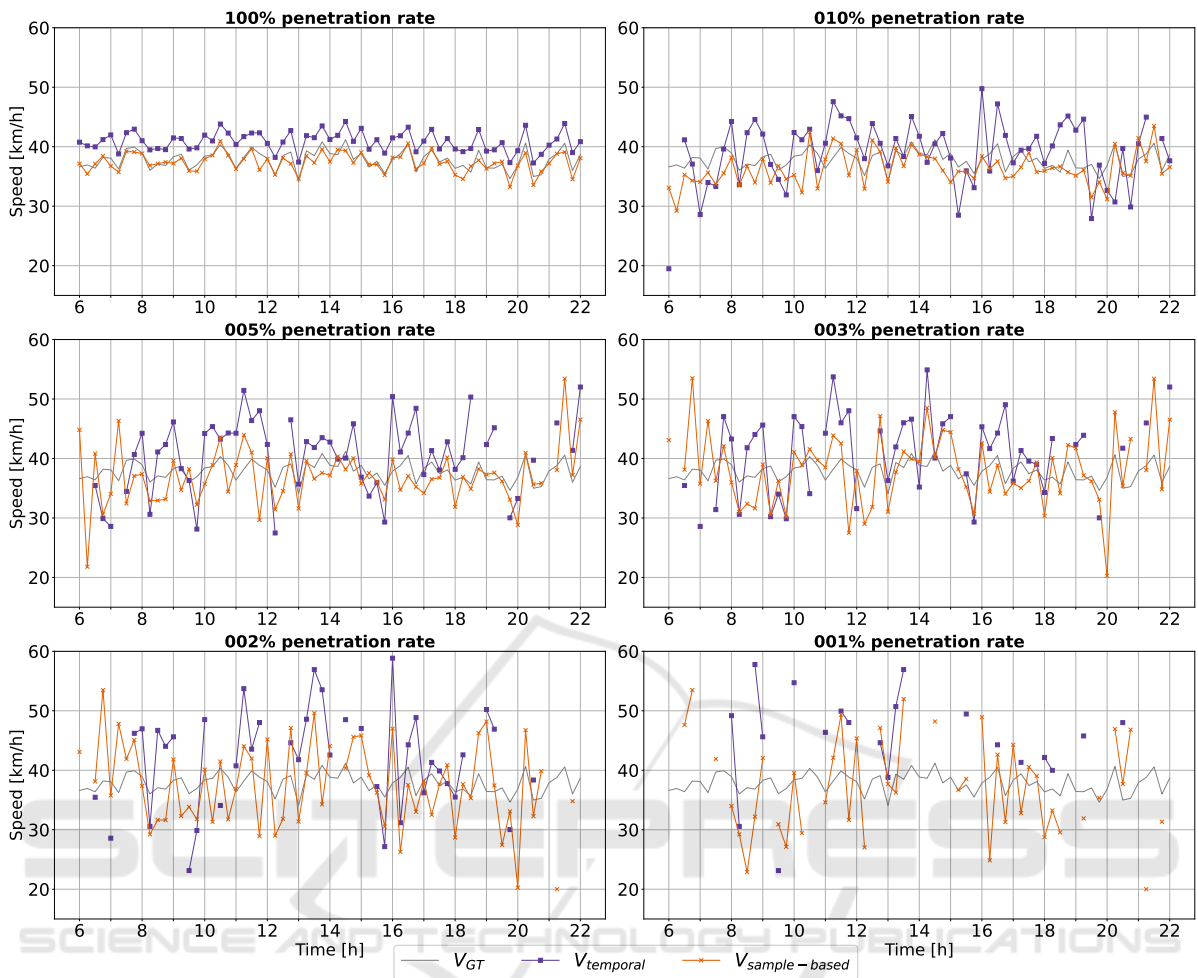


Figure 10: A comparison of the aggregated sample-based mean speed against the temporal mean speed on the Grunewaldstraße. The values are measured for different penetration rates and averaged for 15 min intervals.

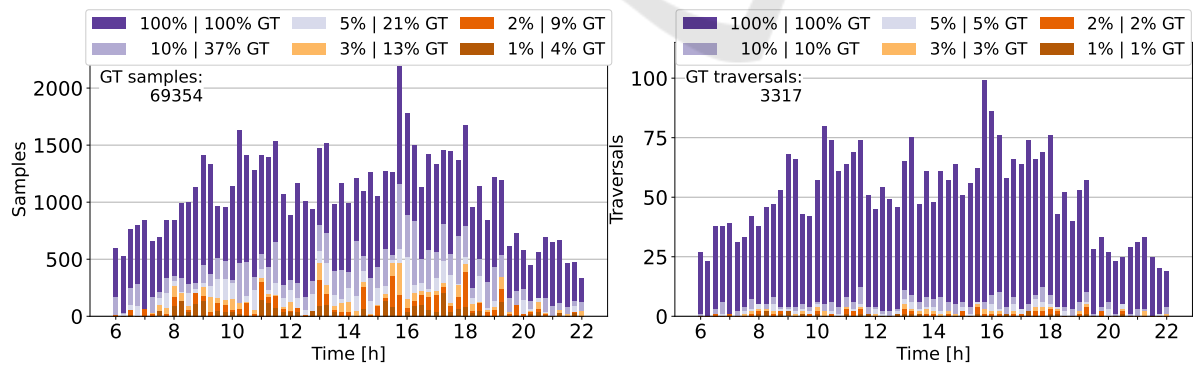


Figure 11: Comparison of received data amount depending on the rate of connected vehicles on the Grunewaldstraße summed-up within 15 min intervals. **Left:** The number of individual samples (i.e., the sum of vehicles per road segment each time step) used for the sample-based mean speed using conventional FCD plus perception. **Right:** The number of extracted traversals used for the temporal mean speed, relying solely on conventional FCD.

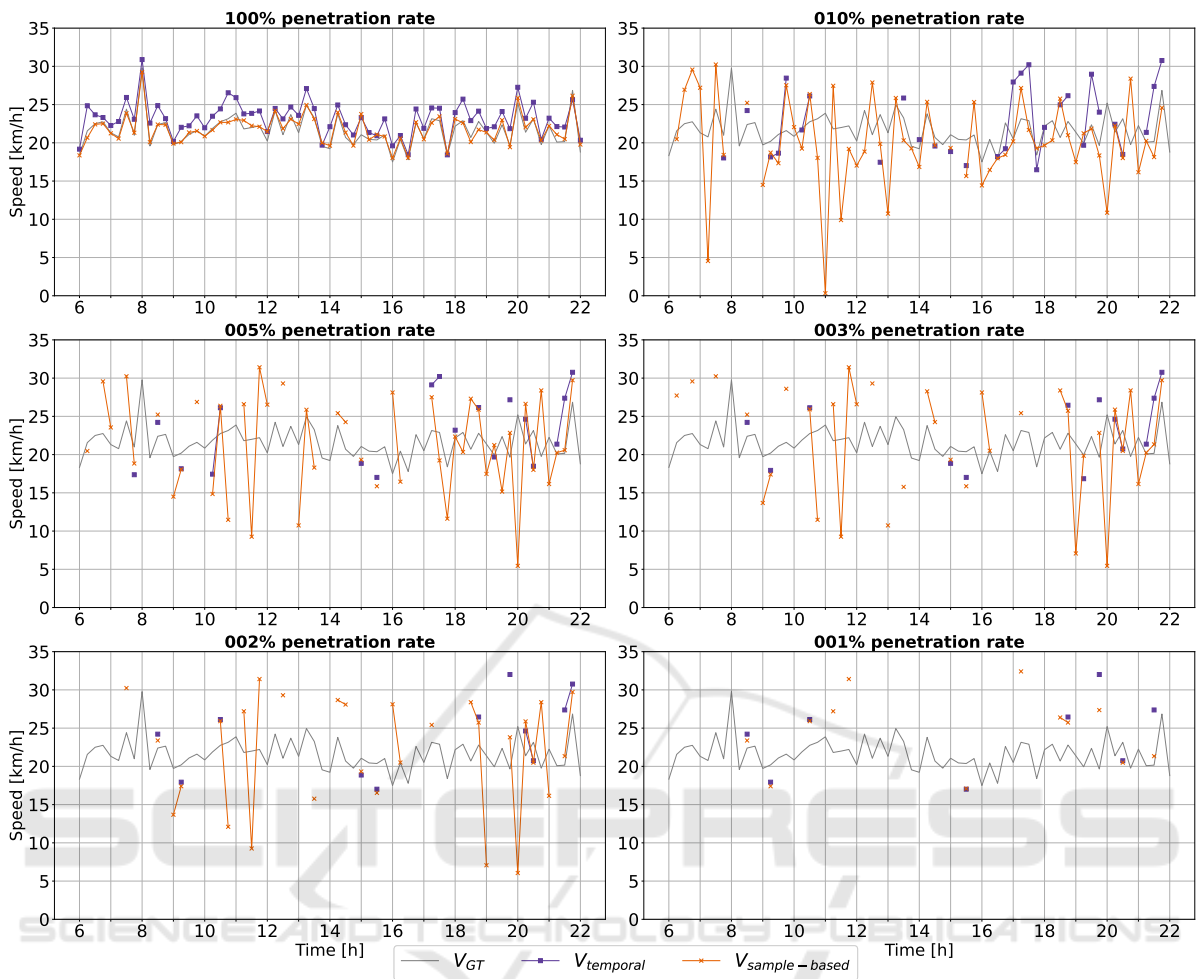


Figure 12: A comparison of the aggregated sample-based mean speed against the temporal mean speed on the Bleibtreustraße. The values are measured for different penetration rates and averaged for 15 min intervals.

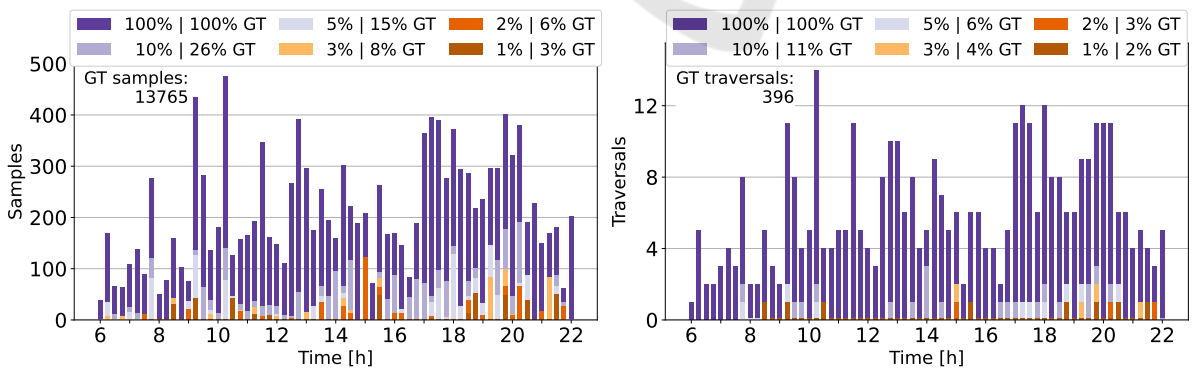


Figure 13: Comparison of received data amount depending on the rate of connected vehicles on the Bleibtreustraße summed-up within 15 min intervals. **Left:** The number of individual samples (i.e., the sum of vehicles per road segment each time step) used for the sample-based mean speed using conventional FCD plus perception. **Right:** The number of extracted traversals used for the temporal mean speed, relying solely on conventional FCD.

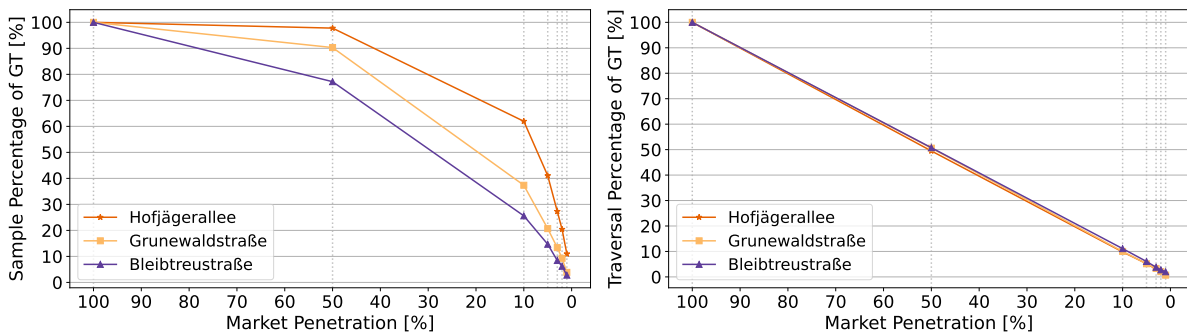


Figure 14: Relation between market penetration and received data points plotted relatively to the GT (i.e., 100 % penetration rate) indicated for penetration rates of 1 %, 2 %, 3 %, 5 %, 10 %, 50 %, and 100 %. **Left:** Plot for the extended FCD. **Right:** Plot for the conventional FCD. Note, the connecting lines are only added for visualization purposes.

With estimates gathered at 1 % only providing marginally better results compared to the temporal mean speed. Looking at the smallest of the three streets, the Bleibtreustraße (Figure 12), some interesting observations can be made. At 10 % market penetration, but also at 5 %, 3 %, and 2 %, some outliers close to 0 km/h are measured. Going back to Figure 3 in Section 2, we can assume that an intersecting CV perceives one or more vehicles waiting at a traffic light with low speeds; thus misrepresenting the estimates for the given time intervals with small speeds. Multiple measures can be taken to get rid of these misinterpretations, a simple approach would be to implement a sample threshold for time intervals, requiring at least n samples before any aggregation happens. Still, when disregarding these outliers, we notice an overall improvement in sample density, decreasing the number of unsampled intervals.

After inspecting the resulting time-series diagrams, we can shift the focus to the underlying data by looking at Figures 9, 11 and 13. Preceding any further evaluation, the difference in significance between *Samples* for the sample-based mean speed and *Traversals* for the temporal mean speed has to be clarified. While a sample is the combined view of a vehicle's position and speed at one point in time, a traversal captures the entire passing of a given road segment, meaning a traversal encodes much more information than a single sample. As a consequence, the magnitude of these values cannot be compared one-to-one, but rather the percentage of data captured compared to the ground truth (here meaning the 100 % penetration rate) is important and therefore additionally displayed in Figure 14. Without the use of perception, the traversal amount is directly proportional to the market penetration on all three road segments, leading to issues on less frequented roads such as the Bleibtreustraße, especially at smaller penetration rates. Looking at the effect of perception, we

can see that there no longer is a linear relation between market penetration and the amount of received data. In fact, on all three roads, the percentages increase over the conventional FCD at all penetration rates. However, a dependence on the road type is apparent once again; the larger the road, the larger the number of additional samples received. This is also very intuitive because the larger a street and its traffic density are, the more likely it is for additional samples to be captured by surrounding vehicle perception, signaling increased samples from *Flowing Traffic*.

In summary, we can see a clear improvement in estimation quality at lower penetration rates due to additional samples being captured by the vehicle perception. Nonetheless, some inconsistencies were identified; when too little of a road segment is being sampled, a misinterpretation of the mean speed may occur. However, this is more likely to happen on smaller, less densely traversed roads, for which a TSE becomes less relevant as these road types rarely experience congestion or other disruptions. Still, being able to accurately measure mean speeds on major road arteries like the Hofjägerallee with small rates of CVs (1 % and smaller) is of great value.

4.2 Travel Time Analysis

After having established that the sample-based mean speed can outperform conventional FCD-based methods in Section 4.1, especially on high-density streets, we aimed at an evaluation proxy for the entire road network. As mentioned previously, mean speed estimates can be used as direct input for routing algorithms, but in addition to choosing better routes, more accurate estimates also enable better calculation of required travel times. In consequence, if we can produce overall more accurate travel time estimates compared to the conventional methods, we can globally assume a better quality of the TSE.

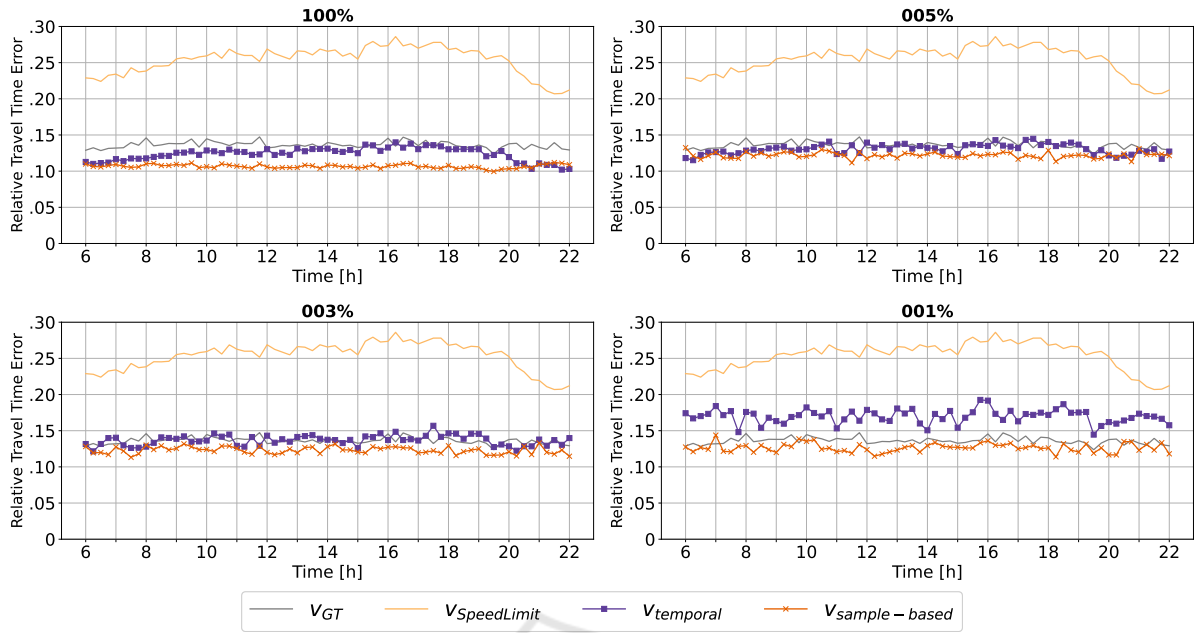


Figure 15: A comparison of the average relative errors between estimated and actual travel times using different mean speed estimates as input for the routing cost.

To test this, we run the same simulation with the same demand twice. The first iteration was used to gather speed estimates, following the methods described in the prior sections. In addition to the temporal and sample-based mean speed, we included the ground truth as well as the speed limit for every road segment. For the second simulation, we developed simple applications that estimate the travel time for their given route by summing up the time it would take to traverse each edge of the route using the described speeds. As the realizable speed also has a temporal dependence, we used the closest available speed estimates not older than one hour before a vehicle started its tour. If no estimate is available the speed limit was used as a default. Also note that no turn costs were considered in the travel time estimation, so a certain bias is to be expected. Results of the estimations as well as the actual recorded travel times are written to a file for later processing, where errors for all vehicles starting their tours within an interval are averaged. We calculate the unsigned mean relative error RME^+ for each of the travel time estimates following Equation (4), where t_{travel} is the measured travel time and $t_{x,\text{est}}$ signifies the applied estimate.

$$RME^+ = \frac{|t_{\text{travel}} - t_{x,\text{est}}|}{t_{\text{travel}}} \quad (4)$$

The outcome is plotted in Figure 15 at penetration rates of 100%, 5%, 3%, and 1% for 15 min intervals. In these plots, an error of 0.1 signifies that on average the travel time estimations are wrong by 10%. We

can see that even when using the measured ground truth speeds we have an average error of about 15%, possibly due to the bias caused by ignoring turn costs. Furthermore, the largest error can be observed for the speed limit, which underestimates travel times, especially with increased traffic density throughout the midday. For estimates generated using the temporal and sample-based mean speed, it can be observed that for all measured penetration rates they both outperform the conventional method of using the speed limit as routing cost. Interestingly, they also *outperform* estimates generated using the ground truth; however, this phenomenon likely occurs due to the inherent bias introduced by the simplified cost calculation.

More important is the comparison of the two estimates with the utilized equipment rate of CVs. While for both estimations the average error increases at lower penetration rates, the perception-induced sample-based mean speed can better compensate for missing samples and provides better travel time estimates at lower penetration rates. This becomes especially apparent when looking at the 1% case where the temporal mean speed estimates more often default to using the speed limit thereby increasing the overall error, while the sample-based mean speed estimates still provide consistent results. Following these results an examination of equipment rates of less than 1% appears to be of interest, unfortunately, these experiments could not be conducted within the scope of this paper.

It is important to not lift these results out of proportion, particularly because we used simplified and over-realistic models for communication and perception. Nonetheless, the potential upsides of enriching FCD with data from perception sensors have been proven and should further be examined.

5 CONCLUSION & OUTLOOK

In this paper, we investigated the research question of whether a good level of Traffic State Estimation (TSE) based on Floating Car Data (FCD) can be realized with sufficient precision, even at low equipment rates, yet with high data quality from perception sensors.

In previous work (Schweppenhäuser et al., 2023), we offered an introduction to established speed metrics for TSE and respective sensor modalities as well as their upsides and shortcomings. The main aspects of this work have been reiterated in the first part of this paper. Floating Car Data approaches have been identified to be the most common source for current-day navigation applications. The *Temporal Mean Speed* (Yoon et al., 2007) was found to be one of the core measures to be estimated from FCD traces using curve-fitted traversals. In contrast to conventional methods, we inspected how perception sensors could be used to improve the data quality for the sake of mean speed estimation. We differentiated three traffic scenarios, *Flowing*, *Oncoming*, and *Intersecting* Traffic that show different levels of potential gain. Based on this, we utilized Eclipse MOSAIC's (Schrab et al., 2023) perception module and showed how data gathered from surrounding vehicles can be used as additional input for mean speed estimation in the form of the *Sample-Based Mean Speed*.

To evaluate the established measures, we set up a simulation-based test, leveraging the strengths of MOSAIC. Building on top of previously published applications¹, we developed a new processor for calculating the sample-based mean speed. By coupling state-of-the-art simulators and utilizing the calibrated large-scale *BeST* scenario (Schrab et al., 2022), we can generate sensible and transferable results.

Focusing on the area of Charlottenburg, we first conducted a study comparing the temporal and sample-based mean speed with the ground truth generated by the traffic simulator Eclipse SUMO. We furthermore identified that estimation quality strongly depends on the road type for both the conventional

and the perception-enriched FCD as well as the market penetration of connected vehicles. Consequently, we looked at time-series plots for the speed estimations and the amount of data received for three exemplary road segments in dependence on penetration rates. We were able to validate the proposed approach of the *Sample-Based Mean Speed* as a sensible method to estimate the mean speed. This analysis further showed that regardless of the targeted road type the perception increases the amount of received data, and thereby improves estimation quality. As a consequence, this indicates that penetration rates of 1 % and lower can be sufficient to provide reliable mean speed estimates for larger road segments. Nonetheless, we also identified shortcomings and less promising results for smaller road segments, which we intend to further investigate in future work.

Evaluating the estimation quality on a global scale is a non-trivial task. Therefore, we defined the resulting travel time estimations as a proxy for the overall TSE quality. Our results indicated that using perception data from surrounding vehicles improves average travel time estimates over conventional FCD, particularly at lower penetration rates, thereby indicating a globally improved estimation quality.

Concerning a real-world deployment of the proposed system, some challenges arise. For one, we heavily simplified the vehicle perception and sensor fusion. Real sensors suffer from occlusion and noise, which reduce sample size and quality. Secondly, we disregarded the constraints of the cellular network. Cell coverage, timing issues, losses, and package sizes are not realistically modeled. Nonetheless, this study still holds meaning as the listed limitations can either be overcome by improved technology or only have a minor impact on final results.

In conclusion, our results indicate that data from vehicular perception sensors can be a valuable addition to the input of Intelligent Transportation Systems such as TSE and should be further researched. In the future, we aim to make our results more quantifiable by improving the realism of the applied perception model, including occlusion and noise. We further aim to investigate how the deployed estimation techniques react to more disruptive traffic patterns like congestion, construction sides, and second-row parking.

ACKNOWLEDGEMENTS

This work was supported by the KIS'M project through the German Federal Ministry for Economic Affairs and Climate Action under grant 45AVF3001E.

¹<https://github.com/mosaic-addons/traffic-state-estimation>

REFERENCES

- Blokpoel, R. J., Krajzewicz, D., and Nippold, R. (2010). Unambiguous metrics for evaluation of traffic networks. In *13th International IEEE Conference on Intelligent Transportation Systems*, pages 1277–1282. IEEE.
- Brakatsoulas, S., Pfoser, D., Salas, R., and Wenk, C. (2005). On Map-Matching Vehicle Tracking Data. In *Proceedings of the 31st International Conference on Very Large Data Bases*, pages 853–864.
- Dahmann, J. S., Fujimoto, R. M., and Weatherly, R. M. (1997). The Department of Defense High Level Architecture. In *Proceedings of the 29th Conference on Winter Simulation*, pages 142–149.
- Delooz, Q., Riebl, R., Festag, A., and Vinel, A. (2020). Design and Performance of Congestion-Aware Collective Perception. In *2020 IEEE Vehicular Networking Conference (VNC)*, pages 1–8. IEEE.
- Ferman, M. A., Blumenfeld, D. E., and Dai, X. (2005). An Analytical Evaluation of a Real-Time Traffic Information System Using Probe Vehicles. In *Journal of Intelligent Transportation Systems*, volume 9, pages 23–34. Taylor & Francis.
- Lopez, P. A., Behrisch, M., Bieker-Walz, L., Erdmann, J., Flötteröd, Y.-P., Hilbrich, R., Lücken, L., Rummel, J., Wagner, P., and Wießner, E. (2018). Microscopic Traffic Simulation using SUMO. In *2018 21st International Conference on Intelligent Transportation Systems (ITSC)*, pages 2575–2582. IEEE.
- Messelodi, S., Modena, C. M., Zanin, M., De Natale, F. G., Granelli, F., Betterle, E., and Guarise, A. (2009). Intelligent extended floating car data collection. *Expert Systems with Applications*, 36(3, Part 1):4213–4227.
- Protzmann, R., Schrab, K., Schweppenhäuser, M., and Radusch, I. (2022). Implementation of a Perception Module for Smart Mobility Applications in Eclipse MOSAIC. In *SUMO Conference Proceedings*, volume 3, pages 199–214.
- Ruppe, S., Junghans, M., Haberjahn, M., and Troppenz, C. (2012). Augmenting the Floating Car Data Approach by Dynamic Indirect Traffic Detection. *Procedia - Social and Behavioral Sciences*, 48:1525–1534. Transport Research Arena 2012.
- Schrab, K., Neubauer, M., Protzmann, R., Radusch, I., Manganiaris, S., Lytrivis, P., and Amditis, A. J. (2023). Modeling an ITS Management Solution for Mixed Highway Traffic With Eclipse MOSAIC. *IEEE Transactions on Intelligent Transportation Systems*, 24(6):6575–6585.
- Schrab, K., Protzmann, R., and Radusch, I. (2022). A Large-Scale Traffic Scenario of Berlin for Evaluating Smart Mobility Applications. In *Conference on Sustainable Urban Mobility*, pages 276–287. Springer.
- Schweppenhäuser, M., Schrab, K., Protzmann, R., and Radusch, I. (2023). Spatio-Temporal Speed Metrics for Traffic State Estimation on Complex Urban Roads. In *International Conference on Simulation Tools and Techniques*. Springer.
- Wardrop, J. G. and Charlesworth, G. (1954). A Method of Estimating Speed and Flow of Traffic from a Moving Vehicle. *Proceedings of the Institution of Civil Engineers*, 3(1):158–171.
- Yoon, J., Noble, B., and Liu, M. (2007). Surface Street Traffic Estimation. In *Proceedings of the 5th International Conference on Mobile systems, applications and services*, pages 220–232.